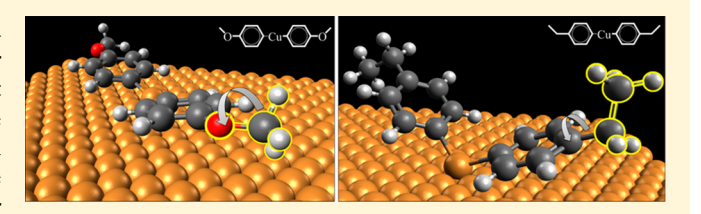
Controlling Molecular Switching via Chemical Functionality: Ethyl vs Methoxy Rotors

Tedros A. Balema,[†] Nisa Ulumuddin,[‡] Colin J. Murphy,[†] Diana P. Slough,[†] Zachary C. Smith,[†] Ryan T. Hannagan,[†] Natalie A. Wasio,[†] Amanda M. Larson,[†] Dipna A. Patel,[†] Kyle Groden,[‡] Jean-Sabin McEwen,*,^{‡,§,||,⊥,#} Yu-Shan Lin,*,[†] and E. Charles H. Sykes*,[†]

Supporting Information

ABSTRACT: Surface-bound molecular rotors provide a useful way to study the structure and dynamics of molecular motion at the single-molecule level. However, when most molecules adsorb on a metal surface, their interaction with the metal changes their properties dramatically, making a priori design impossible. We report a case in which gas-phase predictions of the stable orientations of a class of molecular rotors hold true when they are attached to a surface. This



transferability is achieved by mounting the molecular rotor moiety on a metal—organic complex formed as an intermediate in the surface-catalyzed Ullmann coupling reaction of 1-bromo-4-ethylbenzene versus 1-bromo-4-methoxybenzene. Gas-phase calculations predict that, while the ethyl molecular rotor is most stable when oriented perpendicular to the phenyl ring, the methoxy rotor's stable orientation is in plane with the phenyl ring. Our STM imaging results confirm this behavior, with the methoxy rotor exhibiting switching in plane with the surface versus the ethyl rotor, which switches out of plane with respect to the surface. Furthermore, the two rotors exhibit different rotational excitation characteristics. Action spectra measurements reveal that, while the threshold voltage for direct excitation of the rotational process of the ethyl rotor is identical to the rotational barrier (45 meV), the methoxy rotors require a significantly larger applied voltage (300 mV) than the 128 meV torsional barrier calculated for methoxybenzene in the gas phase. Density functional theory (DFT) calculations of a methoxybenzene molecule on Cu(111) reveal that, while interaction with the Cu(111) surface does not change the preferred orientations of the methoxy rotor, the barrier for rotation is raised to 246 meV, which is much closer to that observed experimentally. This study offers insight into the factors determining the dynamics of molecular rotors based on both the chemical nature of the rotor and its interaction with the surface.

1. INTRODUCTION

Harnessing and controlling the motion of single molecules is a necessity in the fabrication of nanodevices ranging from fluid pumps to microwave signaling applications. ^{1–15} In order to create complex artificial molecular machines, a deep and thorough understanding of their molecular structure and dynamics is required. ^{7,16–26} While mounting molecular machines on surfaces offers the advantage that they can be organized and addressed at the single-molecule level, most often interactions with the surface dramatically alter their properties. Most surface-bound molecular rotors found in the literature tend to be azimuthal, where the axis of rotation is defined as being perpendicular to the surface. ^{9,11–13,27–29} For this geometry, the rotor is in plane and often in close contact

with the surface. Meanwhile, cases of surface-bound altitudinal rotors, being defined as the axis of rotation being parallel to the surface, tend to be relatively few. These rotors operating on different axes will function differently when applied in various devices and offer the potential advantage that the rotor can be switched out of contact with the surface. $^{1-31}$

Using low-temperature scanning tunneling microscopy (LT-STM), we previously examined the formation and surface diffusion of Ullmann coupling intermediates on Cu(111); an example schematic is shown in Figure 1. The reaction was

Received: July 13, 2019
Revised: August 30, 2019
Published: September 3, 2019



[†]Department of Chemistry, Tufts University, Medford, Massachusetts 02155, United States

^{*}Voiland School of Chemical Engineering and Bioengineering, Washington State University, Pullman, Washington 99164, United States

[§]Institute for Integrated Catalysis, Pacific Northwest National Laboratory, Richland, Washington 99352, United States

Department of Physics and Astronomy, Washington State University, Pullman, Washington 99164, United States

¹Department of Chemistry, Washington State University, Pullman, Washington 99164, United States

^{*}Department of Biological Systems Engineering, Washington State University, Pullman, Washington 99164, United States

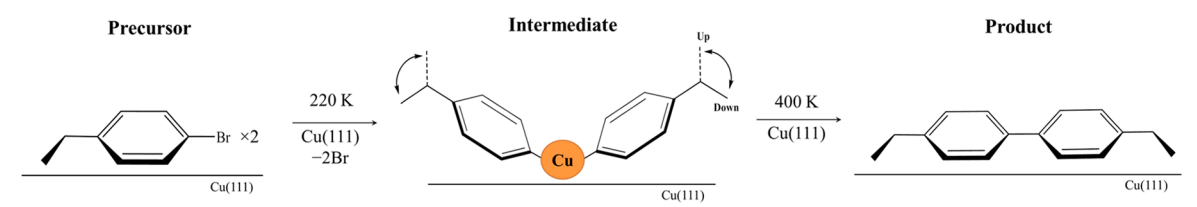


Figure 1. Schematic of the Ullmann coupling reaction of 1-bromo-4-ethylbenzene on Cu(111). The Ullmann coupling intermediate has ethyl groups that rotate. The preferred rotor orientations are indicated with the up—down positions of the ethyl groups.

tracked from the aryl halide reactant, through to metalorganic intermediates, and finally the cross-coupled biphenyl product.³² It was generally found that the aromatic sections of the reactants and the final products laid flat on the surface, but the phenyl groups of the intermediate stage were angled 30-45° off of the surface. 34-36 The intermediates were formed as a Cu atom was removed from the surface, creating a structure that was angled away from the surface with the ethyl rotor in a para position. 31-33,36 The rotation of the C sp²-C sp³ bond of the ethyl rotor of ethylbenzene has been widely studied, and the energies of the conformations in liquid and solid phases have been identified using IR and Raman spectroscopy.³ most stable conformation has the ethyl chain oriented orthogonal to the plane of the benzene ring, while the least stable conformation has the ethyl chain oriented parallel to the plane of the benzene ring.³⁷ The barrier of rotation for the C sp²-C sp³ bond has been calculated to be 40-80 meV depending on the conformation of the ethyl chain.^{37,38} With a dearth of characterization information on ethylbenzene and 1bromo-4-ethylbenzene, it still remains difficult to predict how changing a substituent on the 1-bromo-4-ethylbenzene precursor molecule may impact the rotor dynamics of the intermediates. For example, in terms of small alterations to molecular structure, a previous study found differences in terms of 2D rotor array formation and correlated switching behavior of the Ullmann coupling intermediates on Cu(111) when only one atom of the precursor was different: 1-bromo-4ethylbenzene vs 4-bromo-1-ethyl-2-fluorobenzene.³

In this study, we replace the ethyl rotor group with methoxy to investigate its effects on rotor dynamics. We find that swapping -CH₂- for -O- has a significant impact on the stable orientations of the rotors, their switching dynamics, and molecular interactions with the surface, which results in the different assembly and switching behaviors of the 2D rotor arrays. The most stable conformations of the ethyl rotor are when it is oriented orthogonal to the plane of the benzene ring, as expected from the gas-phase calculations of ethylbenzene. The gas-phase calculation of methoxybenzene indicates that the most stable conformations of the methoxy rotor are when it is parallel to the plane of the phenyl ring. Our results indicate that, in addition to forming different 2D structures, the increased interaction of the methoxy rotor with the Cu(111) surface flattens the metal-organic complex and raises the rotational barrier, but the preferred rotor orientations predicted for the gas-phase molecule are maintained.

2. EXPERIMENTAL METHODS

All LT-STM experiments were performed in an Omicron Nanotechnology GmbH low-temperature microscope, operating under a base pressure of $<1\times10^{-11}$ mbar. The MaTecK Cu(111) single-crystal's cleaning procedure consisted of multiple cycles of Ar⁺ bombardment and 1000 K anneals. Prior to molecular deposition, the cleanliness of the crystal was

determined by STM. Etched W tips were used to record all STM images. 1-Bromo-4-ethylbenzene and 1-bromo-4-methoxybenzene were acquired at 99.9 and 99% purity, respectively, and degassed by multiple freeze/pump/thaw cycles. The 1-bromo-4-ethylbenzene and 1-bromo-4-methoxybenzene were vapor deposited onto a Cu(111) sample held at 5 K through a collimated molecular doser attached to a precision leak valve. Anneals from 5 K were performed in order to equilibrate the molecular ensembles and to initiate the conversion of Ullmann coupling precursor molecules into intermediate structures via removing the sample from the cryogenically cooled stage of the STM and placing it into a sample holder held at room temperature in the UHV chamber for a predetermined length of time. Anneals above 300 K were performed using a resistively heated manipulator arm. The crystal was then cooled back to 5 K by putting it back into the STM stage for high-resolution imaging and spectra collection.

Reflection absorption infrared spectroscopy (RAIRS) experiments were conducted in an UHV chamber with a base pressure of less than 5×10^{-11} mbar. Spectra were collected with a Bruker Tensor II spectrometer and a HgCdTe (MCT) detector. Light was directed from the spectrometer, onto the Cu(111) crystal at a grazing angle, and back out to the detector using a series of gold-coated mirrors encased in a dry air purge box. Chamber windows were made of ZeSe to prevent loss of IR radiation. Spectra were collected with 4 cm⁻¹ resolution, and both the background and the sample spectra were averaged over 2000 scans. Exposures of 1-bromo-4-methoxybenzene (same sample as that described above) were done using a precision leak valve. Spectra were background-subtracted.

3. COMPUTATIONAL DETAILS

The energy of the ethylbenzene molecule was calculated at 10° increments of rotation of the ethyl substituent. The energy of the methoxybenzene molecule was calculated at 1° increments of rotation of the methoxy substituent. 40 The calculations in the gas phase were performed using the Gaussian 09 Software package with the B3LYP functional and the 6-311+ G(d,p) basis set. 40 The dipoles of both ethylbenzene and methoxybenzene were calculated using the ESP charges according to the Merz–Singh–Kollman scheme of the respective atoms, with hydrogens summed into heavy atoms.

The interaction between the methoxy rotor and the underlying Cu(111) surface was quantified by modeling the adsorption of methoxybenzene on Cu(111), where the corresponding density functional theory (DFT)-based calculations were performed within the Vienna ab initio simulation package (VASP). The Projector Augmented Wave (PAW) method was employed for computationally efficient treatment of wave functions of core electrons using the data set released in 2012 for VASP 5.2. Ala, Lectronic exchange and correlation were treated under the Generalized Gradient Approximation

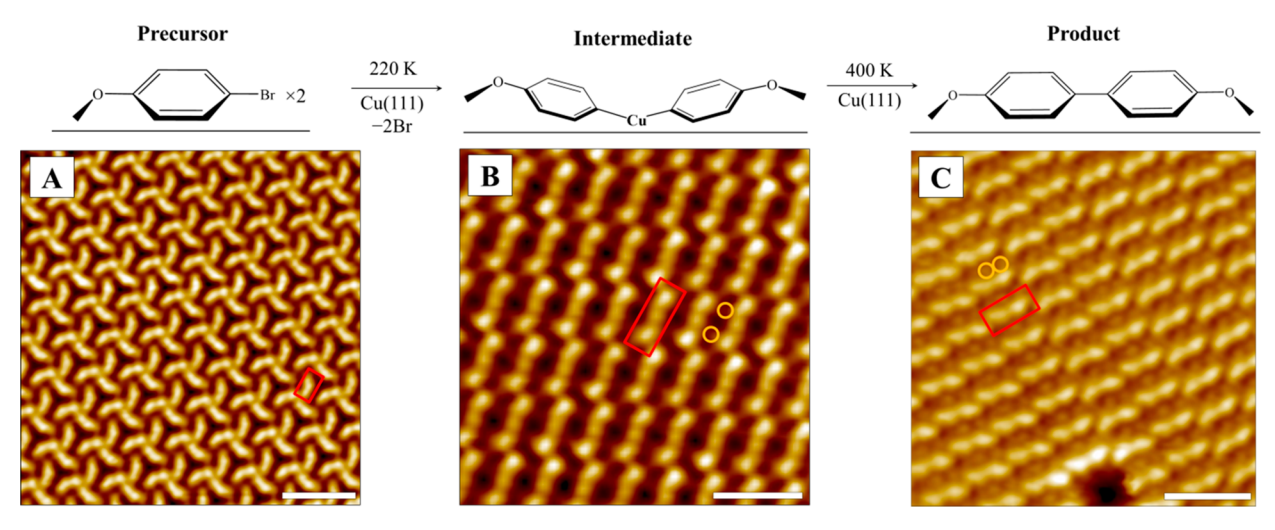


Figure 2. Progression of the Ullmann coupling reaction of 1-bromo-4-methoxybenzene tracked with STM imaging at 5 K on Cu(111). (A) Precursor molecules (1-bromo-4-methoxybenzene) are dosed on a Cu(111) surface and annealed to 120 K. (B) Annealing to 220 K enables C-Br bond cleavage and yields the surface-bound intermediate. (C) Product formation occurs when the intermediates are heated to 400 K. Individual molecules are highlighted within a red box. The orange circles highlight the bromine adatoms. Scanning conditions: (A) +50 mV, 100 pA; (B) +100 mV, 200 pA; (C) +200 mV, 200 pA. Scale bar: 2 nm.

(GGA) using the optb86b-vdW functional, 45 where van der Waals corrections have been included. 46,47 We used a cutoff energy of 500 eV for the plane-wave basis set. The surface was modeled as a p(5 \times 5) Cu(111) surface supercell consisting of four atomic layers with the bottom two layers fixed and a vacuum spacing of 15 Å. A theoretical bulk Cu lattice constant of 3.599 Å was computed through symmetrically constrained optimization of the primitive Cu unit cell (fcc) using a (20 \times 20×20) non- γ -centered Monkhorst-Pack k-point grid, which agrees with previously reported experimental and theoretical values. 45,48 Electronic convergence was considered achieved when the total energy change between subsequent selfconsistent field steps was less than 10⁻⁴ eV.⁴² Geometries of the structures were considered optimized when forces on all relaxed Cartesian degrees of freedom dropped below 0.02 eV/ Å. A $(4 \times 4 \times 1)$ γ -centered mesh was used to sample the Brillouin zone in all slab calculations. The adsorption site of methoxybenzene on Cu(111) was systematically scanned on all possible sites available on Cu(111) and is discussed in the Supporting Information (see Figures S1 and S2). The methoxybenzene on the Hcp 0-C1 site was found to be the most energetically favorable and was chosen as the initial state for the dihedral angle rotation barrier calculation of the methoxy group on the Cu(111) surface.

The dihedral angle rotation barrier was computed using the climbing image nudged elastic band (CINEB) method. Projected force minimizations for all images along this pathway were performed using a simple quick-min algorithm. To verify that the transition state lay on a saddle point, a vibrational mode analysis was performed to ensure that the structure has the required imaginary mode. The convergence criteria for total energy and interatomic forces were set to 10^{-4} eV and 0.03 eV/Å, respectively. A finite difference step size of 0.01 Å was used for the Hessian matrix construction. Charge transfer between the surface and the molecule at each step in the minimum-energy pathway was visualized through a differential charge analysis at isosurfaces of 0.005 and 0.0005 e/Bohr³ in the VESTA 3 software. The charge density difference was calculated according to the expression given in eq 1

$$\Delta n(r) = n_{\text{methoxy+Cu}(111)}(r) - n_{\text{Cu}(111)}(r) - n_{\text{methoxy}}(r)$$
(1)

where $n_{\rm methoxy+Cu(111)}$, $n_{\rm Cu(111)}$, and $n_{\rm methoxy}$ denote the charge density for the methoxybenzene adsorbed on a Cu(111) surface, the Cu(111) slab, and the gas-phase methoxybenzene molecule, respectively.

4. RESULTS AND DISCUSSION

The progression of the Ullmann reaction of 1-bromo-4-methoxybenzene was tracked from the precursor molecules, through the intermediates, to the dimethoxybiphenyl products. This allows for characterization of the relevant steps of the reaction, as shown in Figure 2. Upon deposition onto the Cu sample held at 5 K and annealing to 120 K, 1-bromo-4-methoxybenzene adsorbs in large-scale ordered arrays consisting of a trio of molecules with the bromine groups facing toward the center of the trimer (Figure 2A). The intermediate structure is formed by annealing the sample to 220 K, followed by further cooling to 5 K for imaging (Figure 2B). Further annealing the sample to 400 K yields the final product 4,4'-dimethoxybiphenyl (Figure 2C).

Although there are only slight differences in molecular structure, the domains formed by the 1-bromo-4-methoxybenzene Ullmann intermediates (Figures 2B and 3A) differ greatly from that of 1-bromo-4-ethylbenzene intermediates (Figure 3B). On closer inspection, the individual intermediates of 1-bromo-4-methoxybenzene appear to have either a sigmoid shape (S-shaped; blue box, Figure 3A) or crescent shape (Cshaped; green box, Figure 3A). These shapes directly correspond to the orientation of the methoxy rotors adopting either a cis or trans configuration. Meanwhile, the 1-bromo-4ethylbenzene intermediates have a dumbbell shape, with the ends being either bright or dim, which directly corresponds to the orientation of the ethyl rotor facing away from the surface or toward the surface, respectively (orange box, Figure 3B).31-34 This difference in rotor orientation not only affects how the molecules arrange themselves but also shows how the bound phenyl groups lie. 32-37

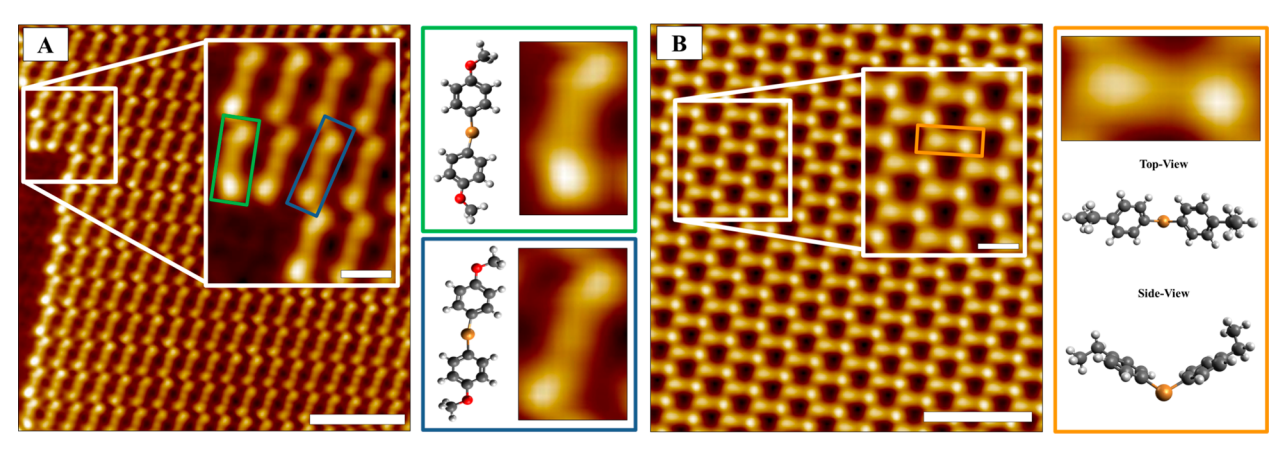


Figure 3. STM images of Ullmann coupling intermediates at 5 K. (A) STM image of a domain of the Ullmann coupling intermediates of 1-bromo-4-methoxybenzene. The inset shows a close-up of a section of the domain, where individual molecules with different methoxy orientations are highlighted in blue and green. The proposed molecular structures, alongside their respective highlighted molecules, are shown in their respective (blue and green) colored boxes on the right. (B) STM image of a domain of the Ullmann coupling intermediates of 1-bromo-4-ethylbenzene. The inset shows a close-up of a section of the domain, where an individual molecule is highlighted in orange. The top- and side-view molecular structure of the individual highlighted molecule is shown in the orange box on the right. Imaging conditions: (A) +100 mV, 50 pA; scale bar: 4 nm; inset scale bar: 1 nm; (B) -10 mV, 10 pA; scale bar: 4 nm; inset scale bar: 1 nm.

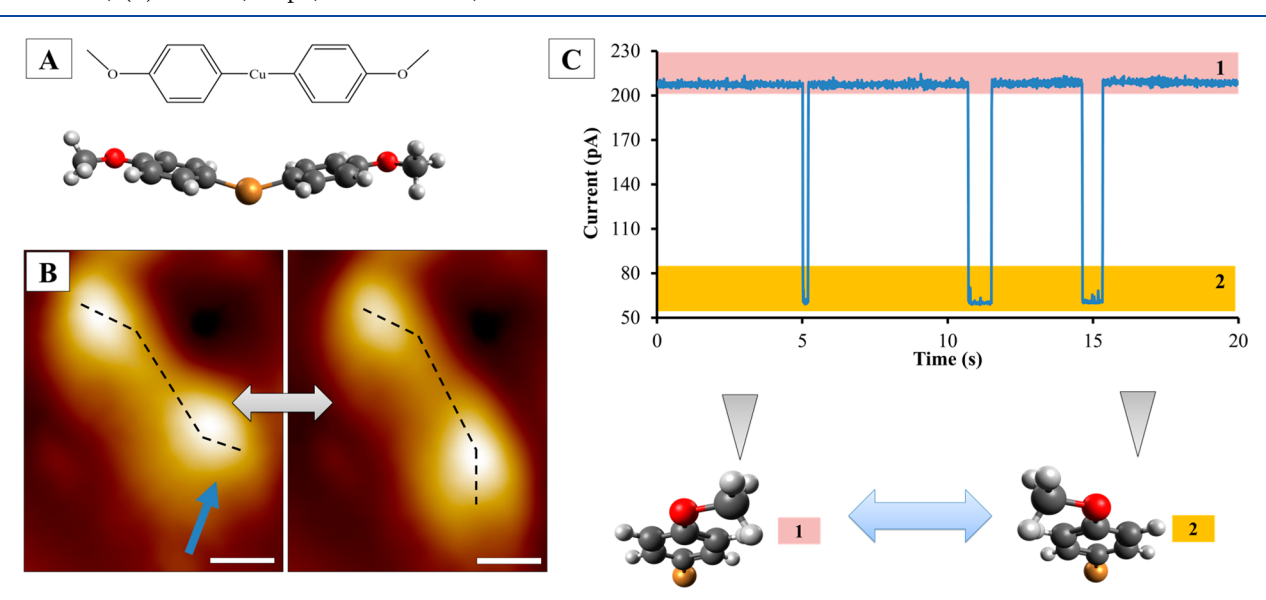


Figure 4. (A) Chemical structure and side-view schematic of the surface-bound intermediate of 1-bromo-4-methoxybenzene. (B) LT-STM images of an individual surface-bound intermediate of 1-bromo-4-methoxybenzene before (left) and after (right) an I(t) measurement, where the blue arrow indicates the placement of the STM tip. The orientation of the molecule is indicated with dashed black lines, for clarity. Scanning conditions: +400 mV, 100 pA. Scale bar: 0.5 nm. (C) I(t) tunneling current vs time trace. The two regions highlighted correspond to the two stable orientations of the methoxy group with respect to the phenyl ring. The two stable methoxy rotor orientations are modeled with the location of the STM tip, below the spectrum. Excitation conditions: +300 mV, 150 pA.

To study the rotational behavior of the Ullmann coupling intermediates, tunneling current versus time experiments (I(t)) were performed. In these experiments, the STM tip was placed next to the extremity of a rotor group of a given molecule isolated from the domains (in this case, either the ethyl or methoxy group). The feedback loop was then turned off, a bias was applied, and the resultant tunneling current was recorded as a function of time. Because the STM tip position and the alignment of the given molecule with respect to the underlying surface did not change, the fluctuations in tunneling current indicate changes in the orientation of the given rotor unit. Figure 4B shows a 1-bromo-4-methoxybenzene intermediate starting off in a trans configuration, and after the I(t) measurement, the intermediate has a cis configuration. The

resulting I(t) trace shows two stable states labeled 1 and 2, respectively, in Figure 4C. These states directly correlate with the observed stable orientations of the methoxy tail, shown in the lower panel of Figure 4C. State 1 shows that the methoxy rotor is orientated toward the tip, thus resulting in a larger current. On the other hand, in state 2, the methoxy rotor is orientated away from the tip, resulting in a drop in current.

When I(t) measurements were performed on the ethyl rotor of the 1-bromo-4-ethylbenzene intermediate, similar observations were made, as shown in Figure 5, albeit the individual up/down states of isolated molecules cannot be seen directly in the STM images. However, the I(t) spectra exhibit two stable states of the tunneling current, consistent with switching between the two most stable orientations of the ethyl rotor:

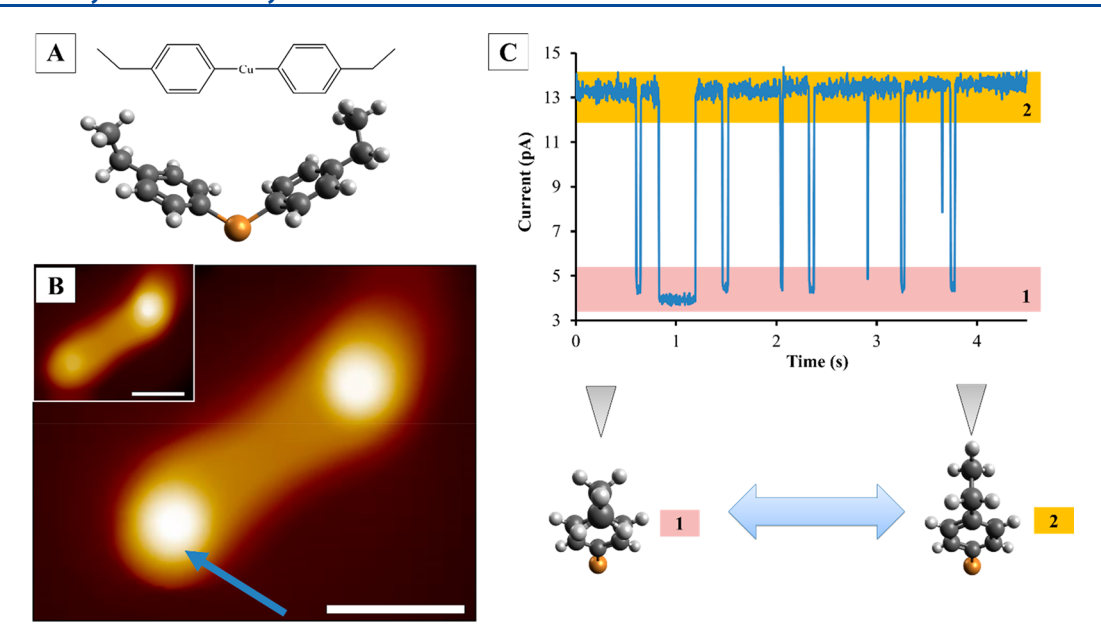


Figure 5. (A) Chemical structure and side-view schematic of the surface-bound intermediate of 1-bromo-4-ethylbenzene. (B) STM image at 5 K of a single molecule of the intermediate with a blue arrow indicating the position where I(t) measurements were taken. Scan conditions: +30 mV, 100 pA. Scale bar: 1 nm. (C) I(t) spectra measurement trace. The two regions highlighted correspond to the two stable orientations of the ethyl group with respect to the phenyl ring. The two stable ethyl rotor orientations are modeled with the location of the STM tip, below the spectrum. Excitation conditions: +50 mV, 5 pA.

either toward or away from the surface. State 1 indicates that the ethyl rotor is oriented away from the tip (down), while conversely state 2 indicates that the ethyl rotor is orientated toward the tip (up).

To understand the molecular origin of the different properties of the two intermediates formed by 1-bromo-4methoxybenzene vs 1-bromo-4-ethylbenzene, theoretical calculations were performed to examine the rotation of the O-C sp³ bond of methoxybenzene and the rotation of the C sp²-C sp³ bond of ethylbenzene in the gas phase (Figure 6A). The rotational barrier is much higher for methoxybenzene, and furthermore, the theoretical calculation of the methoxybenzene rotation differs significantly from that of the ethylbenzene in terms of the location of the energy maxima and minima. These results indicate that the most stable conformations of ethylbenzene are those where the rotors are orthogonal to the plane of the phenyl ring, i.e., the up and down orientations (rotation angles of -90 and 90° ; red dashed line in Figure 6A). The most stable conformations of methoxybenzene, on the other hand, are those where the rotors are parallel to the plane of the benzene ring (rotation angles of 0 and 180°; blue solid line in Figure 6A). In the case of the 1-bromo-4-ethylbenzene, the experimentally measured barriers and rotor orientations match the calculated orientational minima for ethylbenzene as well as the magnitude of the torsional barriers for rotation of the ethyl group. 31,37 The STM switching data collected for the 1-bromo-4-methoxybenzene intermediate are also consistent with the methoxybenzene gas-phase calculation; in that, the methoxy rotors in the STM images lie parallel rather than orthogonal to the surface (Figure 6B).

In order to compare and contrast the excitation mechanism of the ethyl and the methoxy rotors, we performed action spectroscopy. Action spectroscopy is performed by having the feedback loop switched off, where the molecule is excited while its rate of rotation can be monitored by recording changes in the tunneling current. The rotation rate is then measured as a

function of applied bias at a constant tunneling current.⁵² The action spectra in Figure 7A show that the rate of methoxy group rotation is extremely low at biases < 300 mV, whereas above this threshold the rate of rotation increases sharply. The action spectra being symmetrical about 0 V is characteristic of inelastic electron excitation of a molecular vibration that is insensitive to the direction of electron flow.⁵³ Furthermore, when the tunneling current dependence of the rotation rate is plotted for an excitation, voltages at the barrier are consistent for a one-electron process, as shown in the inset of Figure 7B, versus a multielectron process below the barrier.^{53–55} This also supports the mechanism being inelastic excitation of the rotor with a barrier less than 300 meV.

We note that the experimental results for the rotational switching of the methoxy rotor occurs at a larger energy than the calculated gas-phase rotational barrier of 128 meV (Figure 6A). The experimental barrier of 300 meV does not match with any vibrational modes of the methoxy rotor. ^{56–58} Furthermore, in the RAIRS spectra shown in Figure 8, there is an absence of any strong vibrational bands in the 300 meV range (2419 cm⁻¹). It is important to note that the methoxy rotor does not lie completely parallel but rather is slightly tilted off the plane of the surface, as indicated with the presence of the 2895 cm⁻¹ peak corresponding to the symmetric stretch mode of the CH₃ group.

Considering that the STM experiments were performed on lone molecules, there is a lack of lateral interactions to stabilize the orientation of the methoxy rotor, which further points to interactions with the underlying surface having a greater effect. The influence of the Cu(111) surface toward the dihedral rotation barrier of the methoxy group was therefore investigated using a DFT-based model starting from the ground-state configuration of methoxybenzene (the hcp 0-C1 site; see Figures S1 and S2) so as to better rationalize the experimental results. This model also converged with the rotor laying parallel to the surface, which is consistent with the

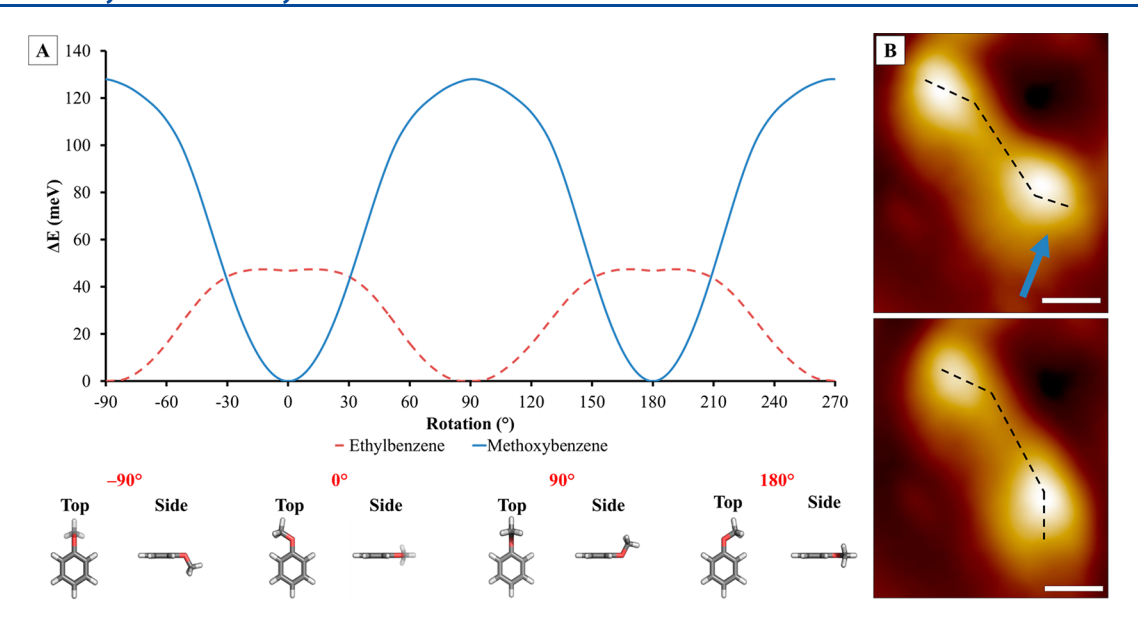


Figure 6. (A) Gas-phase rotational barrier around the O-C sp³ bond of a methoxybenzene molecule (solid blue line). Schematics of conformations at dihedral angles of -90, 0, 90, and 180° from both top- and side-views are shown below the graph. The gas-phase rotational barrier around the C sp²-C sp³ bond of an ethylbenzene molecule is also included for comparison (red dashed line). (B) LT-STM images of an individual surface-bound intermediate of 1-bromo-4-methoxybenzene before (top) and after (bottom) an I(t) measurement, where the blue arrow indicates the placement of the STM tip. The orientation of the molecule is indicated with dashed black lines, for clarity. Scanning conditions: +400 mV, 100 pA. Excitation conditions: +300 mV, 150 pA.

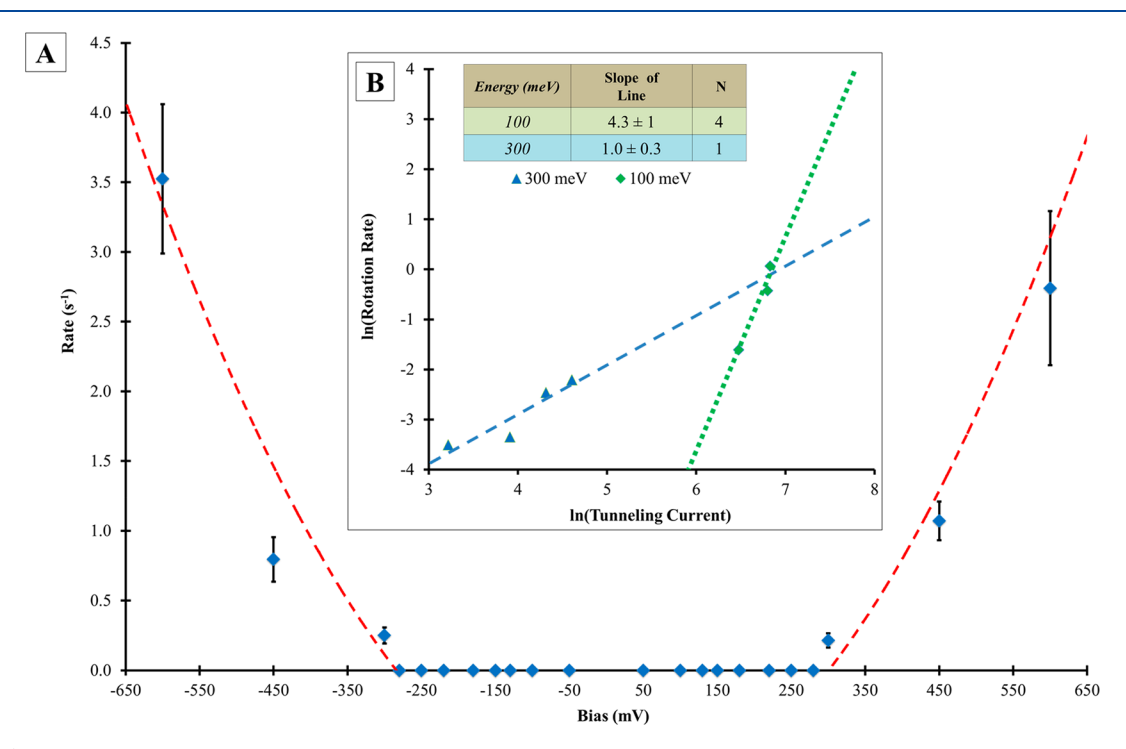


Figure 7. (A) Action spectra for the Ullmann coupling intermediate of 1-bromo-4-methoxybenzene; plot of rotation rate vs bias. (B) Natural logarithm of the rotation rate as a function of the natural logarithm of the tunneling current for various applied electron energies. The lines are power law fits to the data, and the slope of the line, *N*, gives the electron order, i.e., one- vs multiple-electron induced rotation. The power law fits for 100 and 300 meV are indicated with a green dotted line and blue dashed line, respectively.

experimental findings that suggest that the methoxy rotor lies much flatter with respect to the Cu(111) surface than the ethyl rotor system. A 180° dihedral rotation barrier of 246 meV was obtained for the methoxy group, as shown in Figure 9A, which is within DFT error of the experimental value of 300 meV. To understand the influence of the Cu(111) surface on the barrier, a differential charge analysis was conducted, and the calculated

dipole moment of the methoxy bond was compared to that of the ethyl group on their respective molecules.

Through the differential charge analysis shown in Figure 9B, we find no charge transfer at an isosurface of 0.005 e/Bohr³. There is minimal electron transfer between the molecule and the surface even at an isosurface of 0.0005 e/Bohr³. As adsorption sites are all roughly equivalent in energy (Figure

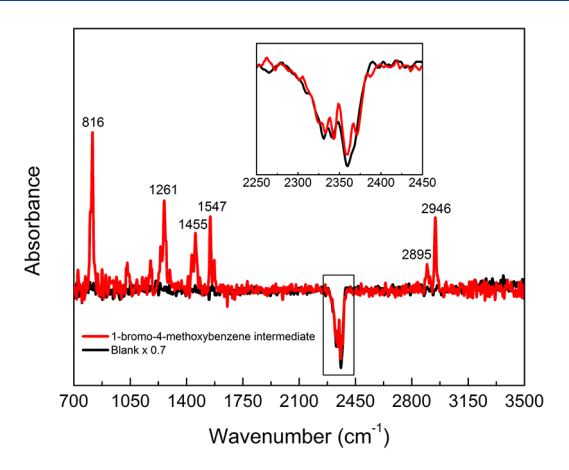


Figure 8. RAIRS spectra for the Ullmann coupling intermediate of 1-bromo-4-methoxybenzene on Cu(111). Spectra collected after a 10 L exposure of 1-bromo-4-methoxybenzene to Cu(111) held at 250 K. A blank spectrum prior to any reactant exposure is included to show similarity of the gas-phase $\rm CO_2$ region, indicating a strong mode due to the coupling intermediate not being present in this region.

S2), we expect that the potential energy surface (PES) of methoxybenzene on Cu(111) is flat. While distinct chemical bonding would be characterized by steep valleys in the PES, a flat one indicates the lack thereof. Furthermore, the bond length between the molecule and the Cu(111) surface was approximately 3 Å, which has been suggested to be typical for physisorption. S9,60 These observations are supported in the literature by a similar conclusion for benzene on Cu(111) and Ag(111) surfaces. Like methyl, we expect methoxy to be a relatively weak activating group. We can thus speculate that the adsorption of methoxybenzene on Cu(111) is dominated by dispersion forces and that the dihedral angle rotation barrier of the methoxy group is not convoluted by chemical bonding between the methoxy group and the surface.

The interaction between the methoxy and ethyl rotors and the Cu(111) surface were examined in terms of dipole—dipole interaction. In our gas-phase calculations, the dipole moment for the methoxy group was 1.95 D, while —0.27 D was obtained for the ethyl group in ethylbenzene. Taking into the account the polarizability of a Cu(111) surface, the much larger dipole of the methoxy rotor, causing a stronger dipole interaction with the surface, may have been the key reason for the higher dihedral rotation barrier as compared to that for the ethyl rotor. This stronger dipole—dipole interaction with the surface could not have been captured through the gas-phase barrier calculation of the methoxy rotor, which rationalizes the previous underestimation of the rotational barrier.

5. CONCLUSIONS

We observed that simply switching the $-\mathrm{CH_2}-$ moiety of an ethyl molecular rotor to $-\mathrm{O}-$ leads to a significant change in rotational behavior in terms of both the stable rotor orientations and the barrier to rotation. The rotor orientations are consistent with the local minima calculated in the respective gas-phase DFT-based calculations, but surface interactions change both the 2D molecular rotor array structure and switching rates. Unlike the ethyl rotor where switching is induced at voltages above 45 meV via a one-electron process (which matches the gas-phase calculations), the methoxy rotor begins switching only at voltages (300 mV) far greater than the gas-phase calculated barrier of 128 meV.

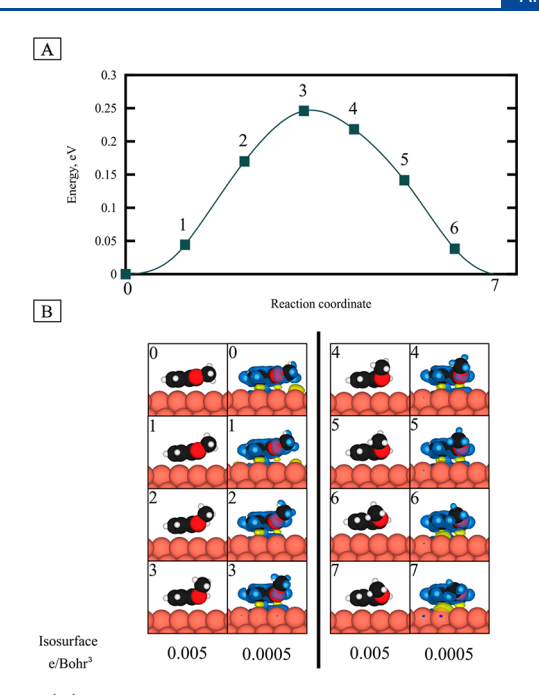


Figure 9. (A) DFT-calculated minimum-energy pathway to rotate the methoxy group of methoxybenzene by 180° when it is absorbed at its most favorable adsorption site. The corresponding images of each number is shown in (B), where 0 and 7 indicate the initial and final states, respectively. Each image is overlaid with isosurfaces of 0.005 (column 1) or 0.0005 e/Bohr^3 (column 2). The blue overlayer represents charge loss, and the yellow overlayer represents charge gain.

This discrepancy is attributed to the greater interactions of the methoxy group with the underlying Cu(111) surface, which serves to increase the torsional barrier but, crucially, does not change its favored conformations. By modeling the adsorption of methoxybenzene on Cu(111), we found with DFT that the phenyl ring and methoxy functional group both lie nearly parallel with the underlying surface, in support of the experimental results. The influence of the surface was deconvoluted by recalculating the rotation barrier of the methoxy group when methoxybenzene is adsorbed on Cu(111). This resulted in a 246 meV barrier, which is much larger than the calculated gas-phase barrier of 130 meV and closer to the experimentally observed 300 meV value. Given that the potential surface energy is flat and charge transfer between methoxybenzene and Cu(111) is poor, we suspect that the molecule interacts with the underlying Cu(111) largely through dispersion forces. The larger dipole of the methoxy rotor (1.95 D) as compared to that of the ethyl rotor (-0.27 D) supports the hypothesis that the dipole-dipole interaction with the Cu(111) surface is stronger for the methyl rotor, resulting in a higher rotation barrier. With an absence of vibrational modes of the rotor complex measured with RAIRS, we postulate that the rotation of the methoxy rotor occurs via direct excitation at the rotational barrier energy (300 meV), and we show experimentally that this is via a one-electron inelastic tunneling process. With this study, we have shed some light on the significance of subtly different chemical moieties in rotary groups of surface-bound Ullmann coupling intermediates and the degree to which their behavior compares with simple gas-phase calculations. This "gas-phase first" approach may prove an effective starting point when designing surfacebound molecular rotors and switches as calculations involving

the large Ullmann coupling intermediates on surfaces are prohibitively computationally expensive. We envision a wider range of molecular switches incorporating other properties such as chirality or rotors tuned with addition of other groups at ortho or meta positions on the phenyl ring that can lead to more complex and controllable switching properties.

ASSOCIATED CONTENT

S Supporting Information

The Supporting Information is available free of charge on the ACS Publications website at DOI: 10.1021/acs.jpcc.9b06664.

Details on DFT investigations of the influence of the Cu(111) surface on the rotation barrier of the methoxy group (PDF)

AUTHOR INFORMATION

Corresponding Authors

*E-mail: charles.sykes@tufts.edu. *E-mail: yu-shan.lin@tufts.edu. *E-mail: js.mcewen@wsu.edu.

ORCID ®

Colin J. Murphy: 0000-0003-0684-2236 Jean-Sabin McEwen: 0000-0003-0931-4869 Yu-Shan Lin: 0000-0001-6460-2877 E. Charles H. Sykes: 0000-0002-0224-2084

Notes

The authors declare no competing financial interest.

ACKNOWLEDGMENTS

The authors thank the U.S. National Science Foundation (Grant CHE-1708397) for support of the experimental work at Tufts, apart from Dr. Amanda Larson who was supported by NSF Grant CHE-1764270. Y.S.L. acknowledges a Tufts start-up fund and the Knez Family Faculty Investment Fund for support of the calculations. Financial support for the theory work at WSU was provided by the National Science Foundation CAREER program under Contract No. CBET-1653561. A portion of the computer time for the computational work was performed using EMSL, a national scientific user facility sponsored by the Department of Energy's Office of Biological and Environmental Research and located at PNNL. PNNL is a multiprogram national laboratory operated for the U.S. DOE by Battelle.

■ REFERENCES

- (1) Astumian, R. D.; Derényi, I. Fluctuation Driven Transport and Models of Molecular Motors and Pumps. *Eur. Biophys. J.* **1998**, 27 (5), 474–489.
- (2) Su, X.; Voskian, S.; Hughes, R. P.; Aprahamian, I. Manipulating Liquid-Crystal Properties Using a PH Activated Hydrazone Switch. *Angew. Chem., Int. Ed.* **2013**, *52* (41), 10734–10739.
- (3) Luo, Y.; Collier, C. P.; Jeppesen, J. O.; Nielsen, K. A.; DeIonno, E.; Ho, G.; Perkins, J.; Tseng, H. R.; Yamamoto, T.; Stoddart, J. F.; et al. Two-Dimensional Molecular Electronics Circuits. *ChemPhysChem* **2002**, *3* (6), 519–525.
- (4) Collier, C. P.; Jeppesen, J. O.; Luo, Y.; Perkins, J.; Wong, E. W.; Heath, J. R.; Stoddart, J. F. Molecular-Based Electronically Switchable Tunnel Junction Devices. *J. Am. Chem. Soc.* **2001**, *123* (50), 12632–12641.
- (5) Kelly, T. R.; Sestelo, J. P.; Tellitu, I. New Molecular Devices: In Search of a Molecular Ratchet. *J. Org. Chem.* **1998**, 63 (11), 3655–3665.

- (6) Anelli, P. L.; Spencer, N.; Stoddart, J. F. A Molecular Shuttle. *J. Am. Chem. Soc.* **1991**, *113* (13), 5131–5133.
- (7) Kay, E. R.; Leigh, D. A.; Zerbetto, F. Synthetic Molecular Motors and Mechanical Machines; 2007; Vol. 46.
- (8) Kottas, G. S.; Clarke, L. I.; Horinek, D.; Michl, J. Artificial Molecular Rotors. *Chem. Rev.* **2005**, *105* (4), 1281–1376.
- (9) Mandl, C. P.; König, B. Chemistry in Motion Unidirectional Rotating Molecular Motors. *Angew. Chem., Int. Ed.* **2004**, 43 (13), 1622–1624.
- (10) Kelly, T. R.; Bowyer, M. C.; Bhaskar, K. V.; Bebbington, D.; Garcia, A.; Lang, F.; Kim, M. H.; Jette, M. P. A Molecular Brake. *J. Am. Chem. Soc.* **1994**, *116* (8), 3657–3658.
- (11) Feringa, B. L. In Control of Motion: From Molecular Switches to Molecular Motors. Acc. Chem. Res. 2001, 34 (6), 504–513.
- (12) Koumura, N.; Zijlstra, R. W. J.; van Delden, R. A.; Harada, N.; Feringa, B. L. Light-Driven Monodirectional Molecular Rotor. *Nature* **1999**, *401*, 152–155.
- (13) Koumura, N.; Geertsema, E. M.; Meetsma, A.; Feringa, B. L. Light-Driven Molecular Rotor: Unidirectional Rotation Controlled by a Single Stereogenic Center. *J. Am. Chem. Soc.* **2000**, *122* (48), 12005–12006.
- (14) Anelli, P.-L.; Asakawa, M.; Ashton, P. R.; Bissell, R. A.; Clavier, G.; Górski, R.; Kaifer, A. E.; Langford, S. J.; Mattersteig, G.; Menzer, S.; et al. Toward Controllable Molecular Shuttles. *Chem. Eur. J.* 1997, 3 (7), 1113–1135.
- (15) Haidekker, M. A.; Theodorakis, E. A. Molecular Rotors Fluorescent Biosensors for Viscosity and Flow. *Org. Biomol. Chem.* **2007**, *5* (11), 1669–1678.
- (16) Coskun, A.; Banaszak, M.; Astumian, R. D.; Stoddart, J. F.; Grzybowski, B. A. Great Expectations: Can Artificial Molecular Machines Deliver on Their Promise? *Chem. Soc. Rev.* **2012**, *41* (1), 19–30.
- (17) Astumian, R. D. Design Principles for Brownian Molecular Machines: How to Swim in Molasses and Walk in a Hurricane. *Phys. Chem. Chem. Phys.* **2007**, *9* (37), 5067–5083.
- (18) Su, X.; Aprahamian, I. Switching around Two Axles: Controlling the Configuration and Conformation of a Hydrazone-Based Switch. *Org. Lett.* **2011**, *13* (1), 30–33.
- (19) Kelly, T. R.; Cai, X.; Damkaci, F.; Panicker, S. B.; Tu, B.; Bushell, S. M.; Cornella, I.; Piggott, M. J.; Salives, R.; Cavero, M.; et al. Progress toward a Rationally Designed, Chemically Powered Rotary Molecular Motor. *J. Am. Chem. Soc.* **2007**, *129* (2), 376–386.
- (20) Eelkema, R.; Pollard, M. M.; Vicario, J.; Katsonis, N.; Ramon, B. S.; Bastiaansen, C. W. M.; Broer, D. J.; Feringa, B. L. Nanomotor Rotates Microscale Objects. *Nature* **2006**, *440* (7081), 163–163.
- (21) Jewell, A. A. D.; Tierney, H. L. H.; Baber, A. E. A.; Iski, E. V.; Laha, M. M.; Sykes, E. C. H. Time-Resolved Studies of Individual Molecular Rotors. *J. Phys.: Condens. Matter* **2010**, 22 (26), 264006.
- (22) Jewell, A. D.; Tierney, H. L.; Zenasni, O.; Lee, T. R.; Sykes, E. C. H. Asymmetric Thioethers as Building Blocks for Chiral Monolayers. *Top. Catal.* **2011**, *54* (19–20), 1357–1367.
- (23) Baber, A. E.; Tierney, H. L.; Sykes, E. C. H. A Quantitative Single-Molecule Study of Thioether Molecular Rotors. *ACS Nano* **2008**, 2 (11), 2385–2391.
- (24) Tierney, H. L.; Murphy, C. J.; Jewell, A. D.; Baber, A. E.; Iski, E. V.; Khodaverdian, H. Y.; McGuire, A. F.; Klebanov, N.; Sykes, E. C. H. Experimental Demonstration of a Single-Molecule Electric Motor. *Nat. Nanotechnol.* **2011**, *6* (10), 625–629.
- (25) Tierney, H. L.; Baber, A. E.; Jewell, A. D.; Iski, E. V.; Boucher, M. B.; Sykes, E. C. H. Mode-Selective Electrical Excitation of a Molecular Rotor. *Chem. Eur. J.* **2009**, *15* (38), 9678–9680.
- (26) Tierney, H. L.; Han, J. W.; Jewell, A. D.; Iski, E. V.; Baber, A. E.; Sholl, D. S.; Sykes, E. C. H. Chirality and Rotation of Asymmetric Surface-Bound Thioethers. *J. Phys. Chem. C* **2011**, *115* (4), 897–901.
- (27) Leigh, D. A.; Wong, J. K. Y.; Dehez, F.; Zerbetto, F. Unidirectional Rotation in a Mechanically Interlocked Molecular Rotor. *Nature* **2003**, 424 (6945), 174–179.

- (28) Hernández, J. V.; Kay, E. R.; Leigh, D. A. A Reversible Synthetic Rotary Molecular Motor. *Science* **2004**, *306* (5701), 1532–1537
- (29) Horinek, D.; Michl, J. Surface-Mounted Altitudinal Molecular Rotors in Alternating Electric Field: Single-Molecule Parametric Oscillator Molecular Dynamics. *Proc. Natl. Acad. Sci. U. S. A.* **2005**, 102 (40), 14175–14180.
- (30) Zheng, X.; Mulcahy, M. E.; Horinek, D.; Galeotti, F.; Magnera, T. F.; Michl, J. Dipolar and Nonpolar Altitudinal Molecular Rotors Mounted on an Au(111) Surface. *J. Am. Chem. Soc.* **2004**, *126* (14), 4540–4542.
- (31) Murphy, C. J.; Smith, Z. C.; Pronschinski, A.; Lewis, E. A.; Liriano, M. L.; Wong, C.; Ivimey, C. J.; Duffy, M.; Musial, W.; Therrien, A. J.; et al. Ullmann Coupling Mediated Assembly of an Electrically Driven Altitudinal Molecular Rotor. *Phys. Chem. Chem. Phys.* **2015**, *17* (47), 31931–31937.
- (32) Lewis, E. A.; Murphy, C. J.; Liriano, M. L.; Sykes, E. C. H. Atomic-Scale Insight into the Formation, Mobility and Reaction of Ullmann Coupling Intermediates. *Chem. Commun.* **2014**, *50* (8), 1006–1008.
- (33) Lewis, E. A.; Marcinkowski, M. D.; Murphy, C. J.; Liriano, M. L.; Therrien, A.; Pronschinske, A.; Sykes, E. C. Controlling Selectivity in the Ullmann Reaction on Cu(111). *Chem. Commun.* **2017**, *53* (111), 7816–7819.
- (34) Nguyen, M. T.; Pignedoli, C. A.; Passerone, D. An Ab Initio Insight into the Cu(111)-Mediated Ullmann Reaction. *Phys. Chem. Chem. Phys.* **2011**, 13 (1), 154–160.
- (35) Jiang, D. E.; Sumpter, B. G.; Dai, S. Structure and Bonding between an Aryl Group and Metal Surfaces. *J. Am. Chem. Soc.* **2006**, 128 (18), 6030–6031.
- (36) Yang, M. X.; Xi, M.; Yuan, H.; Bent, B. E.; Stevens, P.; White, J. M. NEXAFS Studies of Halobenzenes and Phenyl Groups on Cu(111). Surf. Sci. 1995, 341 (1–2), 9–18.
- (37) Fishman, A. I.; Klimovitskii, A. E.; Skvortsov, A. I.; Remizov, A. B. The Vibrational Spectra and Conformations of Ethylbenzene. *Spectrochim. Acta, Part A* **2004**, *60* (4), 843–853.
- (38) Coates, J. Interpretation of Infrared Spectra, A Practical Approach. *Encycl. Anal. Chem.* **2006**, 1–23.
- (39) Wasio, N. A.; Slough, D. P.; Smith, Z. C.; Ivimey, C. J.; Thomas, S. W., III; Lin, Y.-S.; Sykes, E. C. H. Correlated Rotational Switching in Two-Dimensional Self-Assembled Molecular Rotor Arrays. *Nat. Commun.* **2017**, 8 (May), 16057.
- (40) Frisch, M. J.; Trucks, G. W.; Schlegel, H. B.; Scuseria, G. E.; Robb, M. A.; Cheeseman, J. R.; Scalmani, G.; Barone, V.; Mennucci, B.; Petersson, G. A.; Nakatsuji, H.; Caricato, M.; Li, X.; Hratchian, H. P.; Izmaylov, A. F.; Bloino, J.; Zheng, G.; Sonnenberg, J. L.; Hada, M.; Ehara, M.; Toyota, K.; Fukuda, R.; Hasegawa, J.; Ishida, M.; Nakajima, T.; Honda, Y.; Kitao, O.; Nakai, H.; Vreven, T.; Montgomery, J. A., Jr.; Peralta, J. E.; Ogliaro, F.; Bearpark, M.; Heyd, J. J.; Brothers, E.; Kudin, K. N.; Staroverov, V. N.; Keith, T.; Kobayashi, R.; Normand, J.; Raghavachari, K.; Rendell, A.; Burant, J. C.; Iyengar, S. S.; Tomasi, J.; Cossi, M.; Rega, N.; Millam, J. M.; Klene, M.; Knox, J. E.; Cross, J. B.; Bakken, V.; Adamo, C.; Jaramillo, J.; Gomperts, R.; Stratmann, R. E.; Yazyev, O.; Austin, A. J.; Cammi, R.; Pomelli, C.; Ochterski, J. W.; Martin, R. L.; Morokuma, K.; Zakrzewski, V. G.; Voth, G. A.; Salvador, P.; Dannenberg, J. J.; Dapprich, S.; Daniels, A. D.; Farkas, O.; Foresman, J. B.; Ortiz, J. V.; Cioslowski, J.; Fox, D. J. Gaussian 09, revision D.01; Gaussian, Inc.: Wallingford, CT, 2013.
- (41) Kresse, G.; Hafner, J. Ab Initio Molecular Dynamics for Liquid Metals. *Phys. Rev. B: Condens. Matter Mater. Phys.* **1993**, 47 (1), 558.
- (42) Kresse, G.; Furthmüller, J. Efficient Iterative Schemes for Ab Initio Total-Energy Calculations Using a Plane-Wave Basis Set. *Phys. Rev. B: Condens. Matter Mater. Phys.* **1996**, 54 (16), 11169–11186.
- (43) Blochl, P. E. Projector-Augmented Plane-Wave Method. *Phys. Rev. B: Condens. Matter Mater. Phys.* **1994**, 50 (24), 17953.
- (44) Kresse, G.; Joubert, D. From Ultrasoft Pseudopotentials to the Projector Augmented-Wave Method. *Phys. Rev. B: Condens. Matter Mater. Phys.* **1999**, 59 (3), 1758.

- (45) Klimes, J.; Bowler, D. R.; Michaelides, A. Van Der Waals Density Functionals Applied to Solids. *Phys. Rev. B: Condens. Matter Mater. Phys.* **2011**, 83 (19), 1–13.
- (46) Liu, W.; Carrasco, J.; Santra, B.; Michaelides, A.; Scheffler, M.; Tkatchenko, A. Benzene Adsorbed on Metals: Concerted Effect of Covalency and van Der Waals Bonding. *Phys. Rev. B: Condens. Matter Mater. Phys.* **2012**, *86* (24), 1–6.
- (47) Liu, W.; Ruiz, V. G.; Zhang, G. X.; Santra, B.; Ren, X.; Scheffler, M.; Tkatchenko, A. Structure and Energetics of Benzene Adsorbed on Transition-Metal Surfaces: Density-Functional Theory with van Der Waals Interactions Including Collective Substrate Response. *New J. Phys.* **2013**, *15*, 053046.
- (48) Malone, W.; Yildirim, H.; Matos, J.; Kara, A. A van Der Waals Inclusive Density Functional Theory Study of the Nature of Bonding for Thiophene Adsorption on Ni(100) and Cu(100) Surfaces. *J. Phys. Chem. C* **2017**, *121* (11), 6090–6103.
- (49) Henkelman, G.; Überuaga, B. P.; Jónsson, H. Climbing Image Nudged Elastic Band Method for Finding Saddle Points and Minimum Energy Paths. J. Chem. Phys. 2000, 113 (22), 9901–9904.
- (50) Sheppard, D.; Terrell, R.; Henkelman, G. Optimization Methods for Finding Minimum Energy Paths. *J. Chem. Phys.* **2008**, 128 (13), 134106.
- (51) Momma, K. Visualization for Electronic and STructural Analysis (VESTA). http://jp-minerals.org/vesta/en/. (accessed Sep 13, 2019).
- (52) Kim, Y.; Motobayashi, K.; Frederiksen, T.; Ueba, H.; Kawai, M. Action Spectroscopy for Single-Molecule Reactions Experiments and Theory. *Prog. Surf. Sci.* **2015**, *90* (2), 85–143.
- (53) Stipe, B. C.; Stipe, B. C.; Rezaei, M. A.; Ho, W. Single-Molecule Vibrational Spectroscopy and Microscopy. *Science* **1998**, 280, 1732.
- (54) Stipe, B. C.; Rezaei, M. A.; Ho, W. Coupling of Vibrational Excitation to the Rotational Motion of a Single Adsorbed Molecule. *Phys. Rev. Lett.* **1998**, *81* (6), 1263–1266.
- (55) Lauhon, L. J.; Ho, W. Control and Characterization of a Multistep Unimolecular Reaction. *Phys. Rev. Lett.* **2000**, *84* (7), 1527–1530.
- (56) Nakano, H.; Nakamura, I.; Fujitani, T.; Nakamura, J. Structure-Dependent Kinetics for Synthesis and Decomposition of Formate Species over Cu(111) and Cu(110) Model Catalysts. *J. Phys. Chem. B* **2001**, *105* (7), 1355–1365.
- (57) Mudalige, K.; Warren, S.; Trenary, M. Vibrational Analysis of a Chemisorbed Polyatomic Molecule: Methoxy on Cu(100). *J. Phys. Chem. B* **2000**, *104* (11), 2448–2459.
- (58) Degen, I. A. Detection of the Methoxyl Group by Infrared Spectroscopy. *Appl. Spectrosc.* **1968**, 22 (3), 164–166.
- (59) Carrasco, J.; Liu, W.; Michaelides, A.; Tkatchenko, A. Insight into the Description of van Der Waals Forces for Benzene Adsorption on Transition Metal (111) Surfaces. *J. Chem. Phys.* **2014**, *140* (8), 084704.
- (60) Miller, D. P.; Simpson, S.; Tymińska, N.; Zurek, E. Benzene Derivatives Adsorbed to the Ag(111) Surface: Binding Sites and Electronic Structure. *J. Chem. Phys.* **2015**, *142* (10), 101924.
- (61) Yildirim, H.; Greber, T.; Kara, A. Trends in Adsorption Characteristics of Benzene on Transition Metal Surfaces: Role of Surface Chemistry and van Der Waals Interactions. *J. Phys. Chem. C* **2013**, *117* (40), 20572–20583.